MAGIC-TDAS 03-05
030511/RdelosReyes

Effect of earth magnetic field in the MAGIC Telescope effective area for gammas and protons

R delosReyes
<reyes@gae.ucm.es>
J L Contreras
<contrera@gae.ucm.es>
M V Fonseca
<fonseca@gae.ucm.es>

March 5, 2007

Abstract

One of the effects that limits the performance of imaging atmospheric Cherenkov telescopes is the influence of the Earth's magnetic field in the development of extensive air showers (EAS). This effect is due to the Lorentz force exerted in the charged secondary particles (electron and positrons mainly) which are the responsible of the emitted Cherenkov photons. The force, which depends on the local magnetic field of the observation place and the direction where the shower comes from, spreads the Cherenkov light giving as a result a decrease in the number of photons collected by the reflector and a bigger angular dispersion within the image. As a consequence it is expected a higher decrease of the trigger efficiency for gamma detection than for background and therefore the γ effective area of the Cherenkov telescope.

Contents

1 Earth's magnetic field

The Earth is a big spherical magnet, surrounded by its magnetic field. The Earth's magnetic field is a sum of several contributions including the main (core) field, the crustal (anomaly) field, and the external source (magnetospheric) fields. These fields are superimposed on and interacts with each other, but more than 90% of the field measured is generated internal by the Earth's core. This portion of the geomagnetic field is often referred to as the Main Field and dominates the field from the Earth's surface up to about four Earth radii. Beyond that the Earth's magnetic field is increasingly affected by the solar wind interaction with the Earth's magnetosphere.

The Main Field varies slowly in time and can be described by Mathematical Models such as the International Geomagnetic Reference Field (IGRF) and World Magnetic Model (WMM). Magnetic dipoles are used as a first approximation to the electric currents in the Earth's core that are assumed to reproduce the main magnetic field. The model is restrictred to eccentric radial dipoles (North-South poles) at equal distances from the centre of the Earth, but with an offset regarding the geographic poles of around 11 degrees. Within this model it is also included the so called *South Atlantic Anomaly* (SAA)(see figure 1). At a certain location over the South Atlantic Ocean, off the coast of Brazil, the shielding effect of the magnetosphere is not quite spherical but shows a dip, which it is explained as a result of the eccentric displacement of the center of the magnetic field from the geographical center of the Earth (by 280 miles) as well as the displacement between the magnetic and geographic poles of Earth. Above this anomaly the shielding of the Earth's magnetic field decreases, increasing the flux of cosmic's particles.

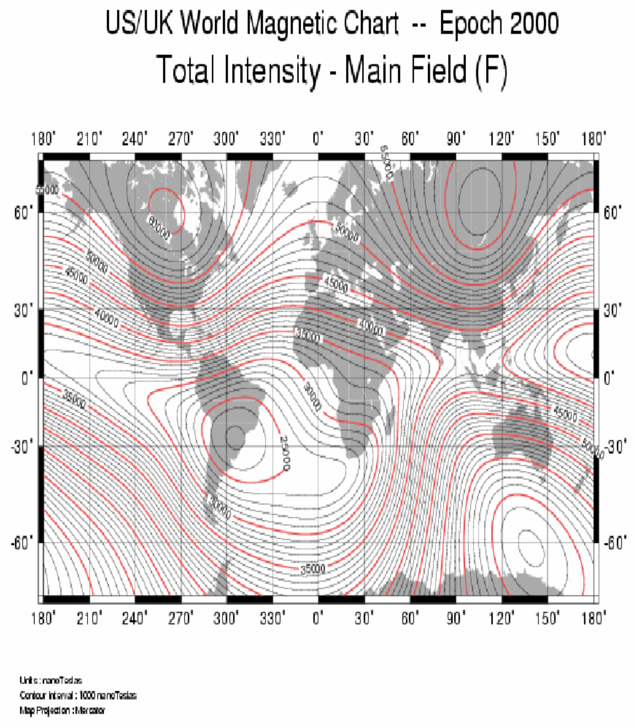

Figure 1: *World magnetic main field (http://www.ngdc.noaa.gov/seg/potfld/WMMImage.shtml).*

At any point, the Earth's magnetic field is characterized by a direction and intensity which can be measured by the magnetic declination (D), the horizontal intensity (H) and the vertical intensity (Z) (figure 2). From these three elements, all other parameters of the magnetic field can be calculated.

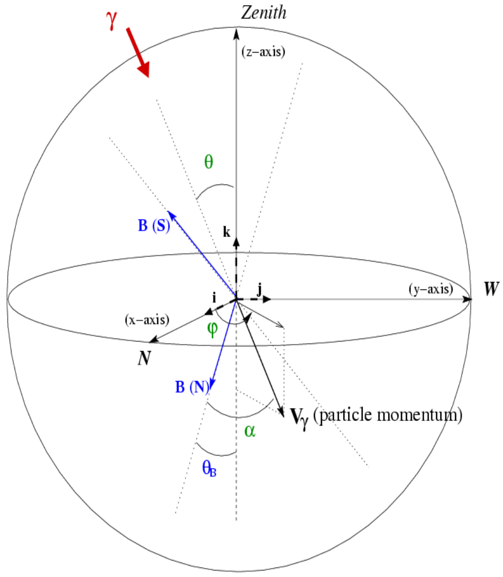

Figure 2: *Coordinate system in CORSIKA [11] and IGRF[1].*

The Earth's surrounding magnetic field exerts a Lorentz force on the secondary charged particles forming an EAS, specifically on the electron/positron pairs (electromagnetic sub-cascades) that give rise to the Cherenkov photons in gamma inittiated showers. This Lorentz force depends on the zenith (θ) and azimuth (ϕ) angles of the gamma showers directions and the local magnetic field intensity. Using the CORSIKA coordinate frame ($\vec{i}, \vec{j}, \vec{k}$), where B_y=0, the values H and Z of the magnetic field parameters corresponds with the two CORSIKA program components B_x and B_z.

$$\vec{F} = \propto q \cdot \vec{B_\perp} \propto \vec{B_\perp} = B_z \sin\theta \sin\phi \; \vec{i} + (B_x \cos\theta - B_z \sin\theta \cos\phi) \; \vec{j} + B_x \sin\theta \sin\phi \; \vec{k} \tag{1}$$

With this expression we can compute the perpendicular component of the magnetic field (or relative Lorentz force) exerted on the electron/positron particles of the shower, as a function of the zenith and azimuth angles of the primary particle direction. It must be remembered that the azimuth angle at CORSIKA reference frame doesn't correspond to the definition of Astronomical azimuth, defined as the angular distance measured towards the East, from North, along the astronomical horizon. The azimuth angle of CORSIKA will be the only one used in this work. Acording to figure 2, the telescope points to the opposite azimuth direction to the particle momentum direction. We will refer to *N,W,S,E* as the telescope directions, which will correspond to ϕ = 180°,270°,0°, 90° on CORSIKA reference frame.

We have calculated the module of $B_\perp$ for the site of La Palma ($B_x = 30.171$, $B_z = 24.227$, $Latitude =$ 28.8). It is represented in color scales, in alt-azimuth coordinates (CORSIKA), in figure 3 and in equatorial coordinates in figure 4. In these figures the color axis on the right represents the ratio of the $B_\perp$ for a given direction to its maximum value.

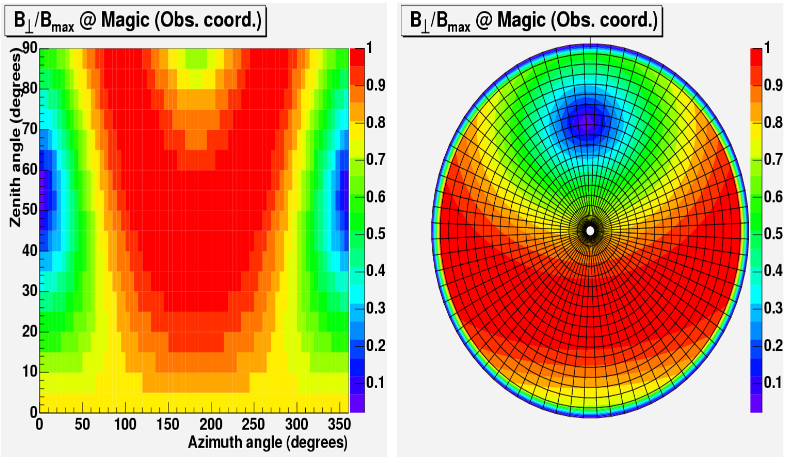

Figure 3: *$B_\perp$ at La Palma for $\theta < 90^o$ (zenith angles above the horizon) in cartesian (left) and polar (right) plots. Azimuth of 0, 90, 180 and 270 degrees correspond to direction of South, East, North and West, respectively.*

From figure 3 we can see that for zenith angles lower than $\sim 39^o$ the maximum effect takes place at the geographic North (azimuth=180^o)(where the angle between the shower and the magnetic field is higher) and the minimum to the South (azimuth=0^o). For $\theta > 39^o$ the situation changes and two maxima appear at both sides of the North, at the East and West directions. The absolute minimum occurs at $\theta = 51^o$ to the South, since this is the zenith angle at which the magnetic field points to for La Palma location ($\Theta = \arctan B_x/B_z$). When the telescope points close to the zenith ($\theta \sim 0^o$) there is no difference among azimuth directions.

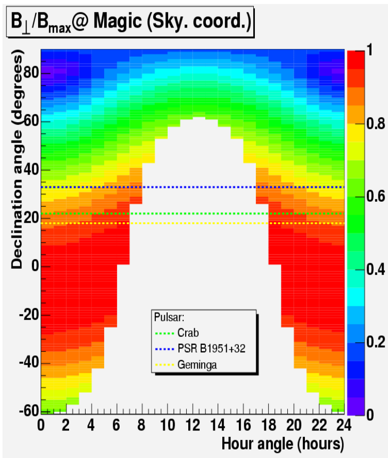

Figure 4: *$B_\perp$ in equatorial coordinates for $\theta < 90^o$. The source culmination takes place at $h = 0^o$*

In figure 4 we have represented again the relative value of $B_\perp$ ($B_\perp/B_{max}$) but in equatorial coordinates. We can see that the magnetic field changes very little along the source trajectory ($\sim 10\%$), however it depends more strongly on declination of the source. In this way the maximum effect takes place for sources with declination between [-20,20] degrees while the minimum occurs for high declination sources, around 80 degrees.

As a comparison we have calculated the value of the perpendicular component of the Earth's magnetic field for different gamma observatories in different Earth places (figure 5). In table 1 we present the four most important future gamma observatories and a proposed one, 5@5 in the Atacama desert [7], together with their coordinates and the values of its horizontal and vertical magnetic field components as well as its polar angle. These numbers have been calculated using the Geomag program [1].

	ϕ (º ' ")	L (º ' ")	h (km)	B_x (μT)	B_z (μT)	Θ (º)
MAGIC [2]	28 45 34 N	17 52 34 W	2.2	30.161	24.245	51.2
HESS [3]	23 16 18 S	16 30 00 E	1.8	12.436	-25.872	25.7
VERITAS [4]	31 40 51.4 N	110 52 39 W	2.32	25.239	40.962	31.6
CANGAROO [5]	31 5 56 S	136 47 10 E	0.16	25.597	-51.612	26.4
5@5 [6]	23 18 00 S	68 09 00 W	5.0	22.220	-7.945	70.3

Table 1: *Location, magnetic field components and angle for five different gamma observatories.*

The difference in the magnetic field due to the altitude is very small, around 0.1% between MAGIC and 5@5 altitudes.

Comparing figure 5 and table 1, we can see that the minimum effect takes place at the culmination of the source while the maximum effect, which depends on the B_z strength, takes place in those directions where the particle momentum is perpendicular to the magnetic field. From figure 5 we can see that in the case of Veritas, for low zenith angles the effect is similar as the one for Magic but for zenith angles higher than 40-50 degrees the effect increases around 30%. We can see that the maximum value of the magnetic field takes place at Cangaroo observatory and the minimum is at 5@5 site. The minimum at the 5@5 location is due to the South Atlantic Anomaly (SAA), a region of lower magnetic field . As a consequence of the lower value of the B_z component of the local magnetic field, the gamma observatories close to this anomaly will have more collected photons into their reflectors as well as an increase of the charged particles rate. For this reason we can not bet for an increase of the telescope sensitivity for the gamma observatories closest to the SAA.

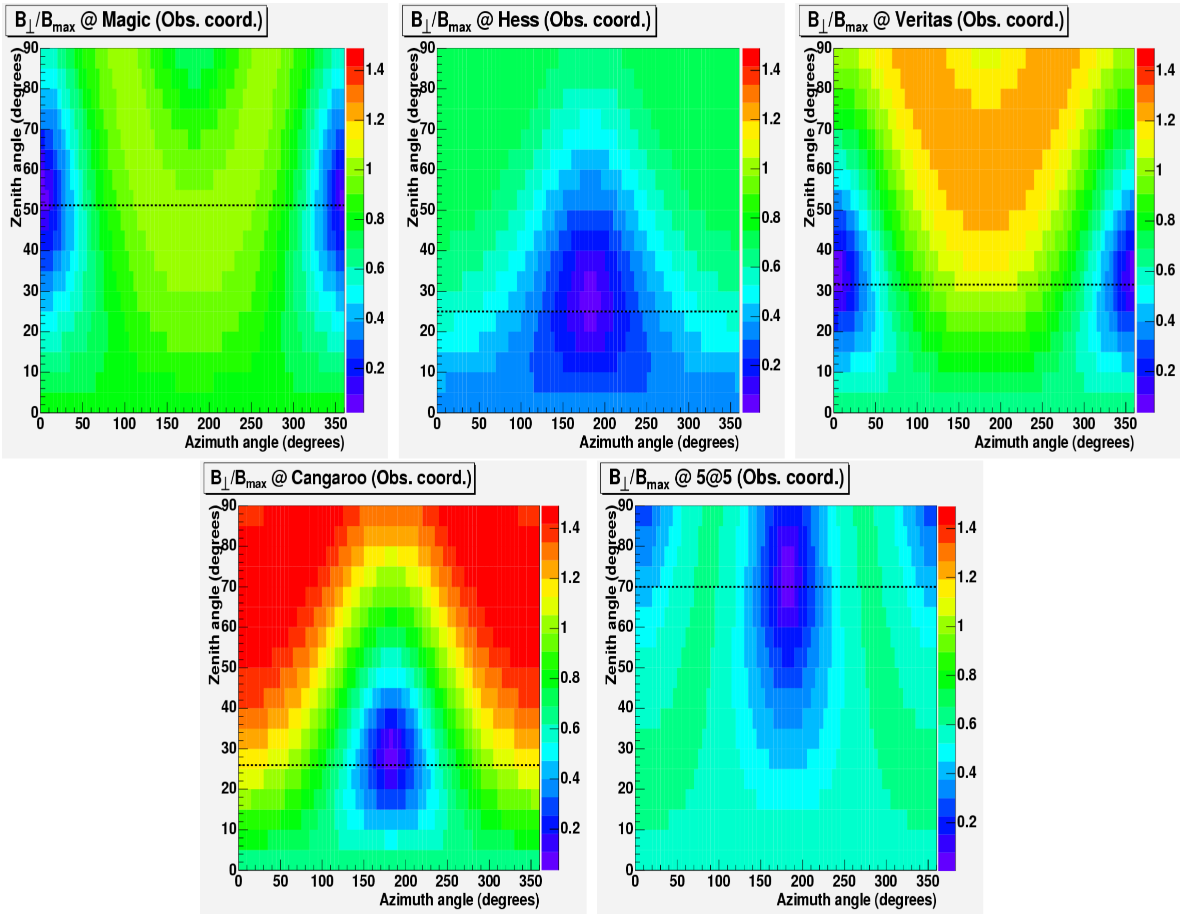

Figure 5: *$B_\perp$ for different observatories: MAGIC, HESS, VERITAS, CANGAROO and 5@5 for $\theta < 90^o$, normalized to the maximal MAGIC value. The dotted line correspond to the zenith angle at which the effect is minimal.*

2 The MC simulation

As a first approximation we have worked at CORSIKA level, instead of making the studies with the events generated by the MAGIC collaboration and the Reflector and Camera simulation programs. We can get thus an idea of how the magnetic field at ground level affects the effective area in the North and South direction, within a reasonable computing time.

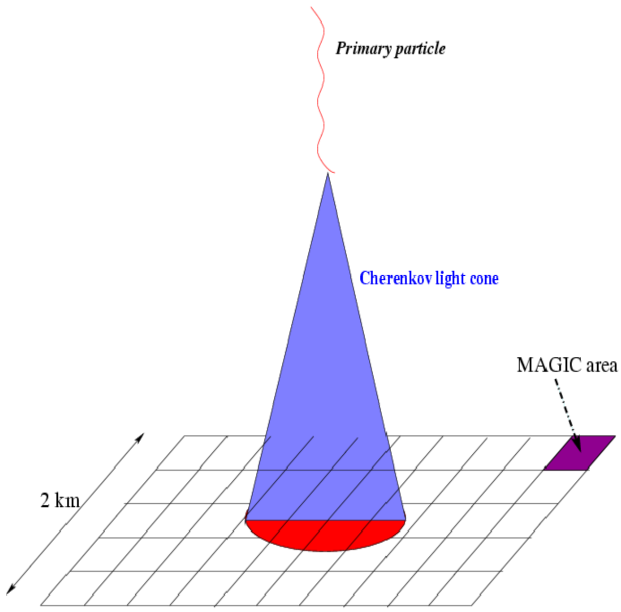

Figure 6: *Scheme of CORSIKA simulation area.*

We have proceeded as follows. We have recorded the Cherenkov photons produced by CORSIKA for each simulated event over a big area ($2 \times 2\ km^2$). We have then divided this area in squares with the MAGIC reflector size ($\sim 236\ m^2$) (see figure 6).

To compute the lateral distributions we just simply sum all the photons collected by each square and divide it by the number of generated events.

In the case of the effective area we have to calculate, first the trigger efficiency for each distance bin and then multiply it by the bin's area. The trigger efficiency is calculated as the number of squares with a number of photons higher than the trigger condition divided by the total number of squares averaged over several events. Multiplying the trigger efficiency by the area considered at ground we get the effective area. We use as approximate trigger condition, the standard one *4mV and 4NN*. We demand a minimum number of Cherenkov photons. Considering a QE=20% (last performance), that 1mV $\sim$ 2 phe/pixel, a multiplicity of 4 (not included the Next Neighbor (NN) topological condition), and a reflectivity of 90%, we have taken ~ 200 photons as the minimum number of Cherenkov photons that trigger the telescope. These photons have to fulfill an angular restriction, since the high energy showers could pass the previous trigger condition in the outer part of the camera which it is not defined as trigger region ($> 0.8^o$-1^o)(see figure 7), for that reason we have only considered the Cherenkov photons within a trigger radius of 1^o from the telescope axis.

Figure 8 shows the angular distribution of Cherenkov photons in the camera plane. The chosen value for the trigger radius is quite wide that it always includes the maximum of the distribution of the

Cherenkov photons. It can be also seen that the "hump" of the distribution moves towards the outer part of the camera for increasing energies being $\leq 1^o$ for energies of 100 GeV (the highest value in our simulation). The "hump" moves towards the center of the camera with increasing zenith angle. We would like to remark that this last behavior is the opposite one to the expected for the lateral distribution, as we will see in the section 3, figure 9.

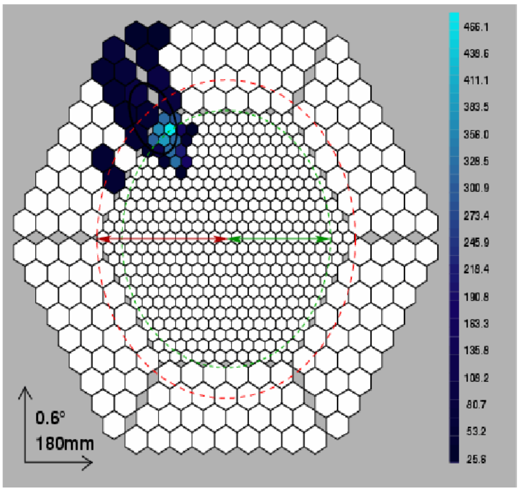

Figure 7: *Camera trigger regions of 1° (green) and 1.3° (red).*

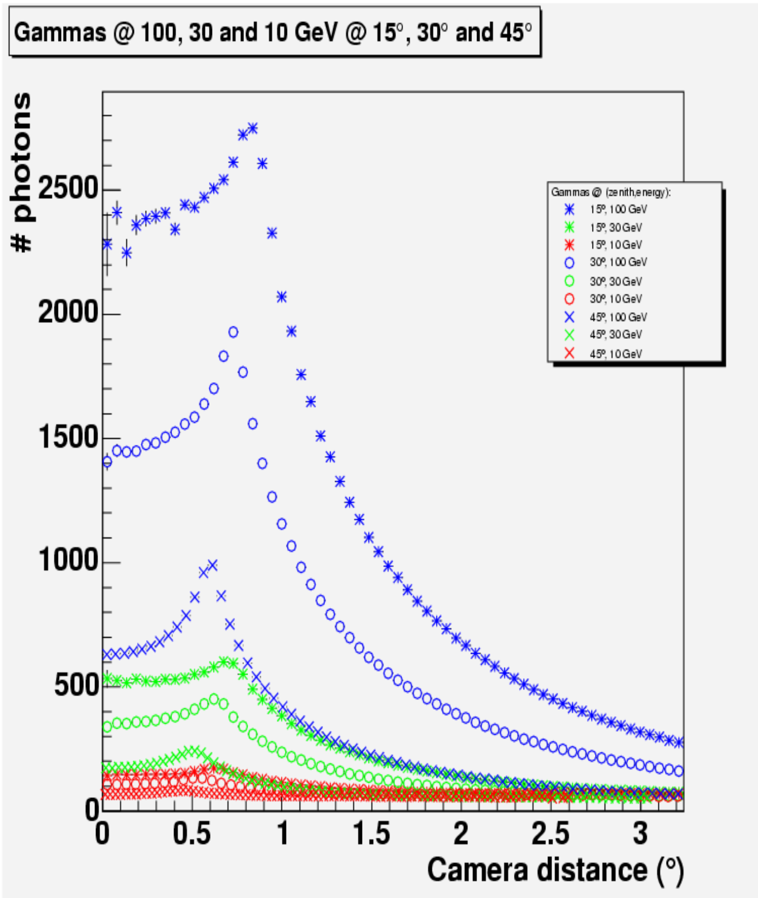

Figure 8: *Distribution of Cherenkov photons in the camera plane for 10 (lowest), 30 and 100 (higher) GeV and zenith angles of 15, 30 and 45 degrees.*

3 Gammas

3.1 Lateral distributions

In this section we show the effect of the magnetic field on the distribution of Cherenkov light for gammas at low energies at MAGIC's site (La Palma). We have worked at CORSIKA level (version 6.19), generating events for different energies, zenith and azimuth angles ϕ=0 (South) and 180 (North) degrees. The statistics of the samples are collected in table 2.

For each set of events we have computed the average lateral (figure 9) and ground (figure 10) distributions of Cherenkov light density.

Energy / Zenith angle	Number of events 15 ^{o}	30^o	45^o
10 GeV	10^4	10^4	10^4
30 GeV	10^4	10^4	10^4
100 GeV	10^3	10^3	10^3

Table 2: *Number of gamma showers generated for each azimuth angle (North and South) as a function of energy and zenith angle.*

As we saw in the $B_\perp$ plot for MAGIC (figure 3) the influence of the magnetic field is minimal at the culmination of the source (North) and maximal at the South (except for the highest zenith angles), so in first approximation we are only concerned with the difference between both extreme cases for zenih angles up to 50^o. The lateral distributions obtained are shown in plots of figure 9.

In figure 9 we can see the lateral distribution for gammas of 10, 30 and 100 GeV for zenith angles of 15^o,30^o and 45^o for North and South directions. On the left plots we see that, in general, the density of Cherenkov light decreases with the energy and the observation altitude for both latitude directions, as it was expected. But in all the cases the Cherenkov photon density is lower for gammas coming from the North that from South direction. This difference between both directions depends on the energy and the zenith angle of the incoming particle. The difference between South and North increases with zenith angle and decreases with energy. For gamma showers at 100 GeV the difference is up to 20% at 45^o while at 15^o there is almost no difference due to the higher momenta of the charged particles (see right plots in figure 9). For the lowest energy showers, those of 10 GeV, the difference increases from 10% at 15^o up to 50% for zenith angles of 45^o. This results are what we expected from the expression 1, where the value of the perpendicular component is proportional to the particle velocity, and figure 3 concerning the dependence with the particle direction. From this results we can expect that the maximum difference takes place to zenith angle of around 51^o for low energies.

As we have commented before, events coming from the South have a higher density of Cherenkov light. This happens for impact parameter range of 0-800 meters approximately. On the left plots of figure 9 we can see that this tendency changes for impact parameter larger than around 1000 meters. We know that the charged component of gamma-initiated EAS are the electromagnetic sub-cascades. This means that all the light lost is due to the effect of the Earth's magnetic field in the electron-positron pairs of the gamma-showers. Therefore we can conclude that the Cherenkov photons spread out by the Earth magnetic field are not recovered inside the Magic telescope effective area (r $\sim$ 180 m) and most of the light lost at low impact parameters is spread out at impact parameters of 1-2 km and higher values.

In figure 9 we have seen the integrated light density at different impact parameter. But, due to the dependence of the magnetic field with the particle direction, it is expected that the magnetic field also affects the shape and size of the EAS ground distribution. This distribution has been represented in figures 10, 11 and 12 for EAS simulated with B and no B. Beacuse CORSIKA program doesn't allow null values for magnetic field component we have had to apply very small values ($B = 0.1\mu$T). These distributions are refered to the telescope reference frame ($\vec{i}\,'$,$\vec{j}\,'$,$\vec{k}\,'$) which rotates around the z-axis (see figure 2) an angle ϕ respect ot the ground reference frame ($\vec{i}$,$\vec{j}$,$\vec{k}$).

In figure 10 we see the ground distribution of Cherenkov photons for gamma showers of 10, 30 and 100 GeV at zenith angle of 15^o (on the top) and 45^o (on the bottom) for different pointing directions, S(ϕ=0), E(ϕ=90), N(ϕ=180) and W(ϕ=270). The color scale plots correspond to EAS simulated with La Palma magnetic field values and the contour lines plots are the corresponding ones where no non magnetic field has been applied. All of them are normalized to the maximum value (displayed as a label in the first plot) of the distribution in the South direction ($\phi = 0$) where the minimum effect of the magnetic field is expected.

In these plots we have to distinguish between two effects: one geometrical, due to a change of reference frame and the other due to the real effect of the Earth's magnetic field onto the EAS images.

The first one can be clearly seen looking to the contour plots, where non-magnetic field has been applied. In these plots the image remains very similar for different azimuth angles and energies for the same zenith angle. If we compare between zenith angles we see that the EAS image enlarges along the figure x-axis while we increase the zenith angle from 15^o to 45^o. This enlargement of the image produces a lost on the light collected by the telescope. The lost is important for high zenith angles and it is the same along the source trayectory while we change on azimuth angle. This effect is due to a geometrical effect of the EAS projected into the telescope reference frame, which is the frame corresponding to the plots of figure 10, and not the ground reference frame. This effect it is also included, although not so clearly seen, into the case if we include the magnetic field into the EAS simulations.

The second effect corresponds to the distortion of the EAS images because of the Earth's magnetic field effect. To understand this effect we have to project the perpendicular component of the magnetic field, given by equation 1, into the telescope reference frame ($\vec{i}\,'$,$\vec{j}\,'$,$\vec{k}\,'$). This is given by equations 3.1, which are the effect of the Lorenz force for different azimuth directions (ϕ= 0,90,180 and 270).

$$\vec{F} \propto -q \cdot v \cdot \begin{cases} (B_x \cos\theta - B_z \sin\theta)\ \vec{j}', & \phi = 0 \text{ (S)} \\ B_x \cos\theta\ \vec{i}' - B_z \sin\theta\ \vec{j}' + B_x \sin\theta\ \vec{k}', & \phi = 90 \text{ (E)} \\ -(B_x \cos\theta - B_z \sin\theta)\ \vec{j}', & \phi = 180 \text{ (N)} \\ -B_x \cos\theta\ \vec{i}' - B_z \sin\theta\ \vec{j}' - B_x \sin\theta\ \vec{k}', & \phi = 270 \text{ (W)} \end{cases} \tag{2}$$

If we have a look to the plot on the top (15^o) of zenith angle) we can see only this second effect, because the first one is not so important. In this plot we see that the EAS images are enlarged along the vector on the x-y plane of the equations 3.1. For azimuth angles 0 and 180 the enlargement is along the y-axis while for aimutal angles of 90 and 270 the enlargement axis form an angle $\tan\alpha = B_z/B_x \tan\theta$ with the x-axis. For zenith angle of 15^o it is around 12^o, while for zenith angle of 45^o it is around 40^o. As well as in the case of the geometrical effect the enlargement of the EAS images, due to the spread of the charged particles by the Earth's magnetic field, causes a lost of the light collected by the telescope. As we can see from color scale plots in figure 10 the amount of light lost is different depending on the azimuth angle because the light is spreaded by the magnetic field in different directions depending on the direction the telescope is pointing to.

For EAS at 45^o of zenith angle, the magnetic field and the geometrical effect are superimpossed. In this case, if we calculate the ratio between the maximum of light density between 45^o and 15^o we should have a decrease of around 50%. If we calculate the same ratio for EAS simulated without B field we get a decrease of around 30%. This lead us to conclude that around 20% of the light lost in the telescope reflector is due to the magnetic field effect, while 30% is due to the spread of the EAS image because of the observation zenith angle.

From equations 3.1 we can see that the image enlargement caused by the magnetic field depends on the directions we are pointing to but also on the particle charge (q) and momentum (v) of the secondary chaged particles of the EAS. The effect of the particle momentum is clearly seen in figure 10 on the light distributions for different energies of the primary γ-ray. If we compare the shower images of 100 GeV with 10 GeV and 30 GeV gamma-showers we can see the the light collected by the telescope decrease with the energy with hardly no effect over the 100 GeV gamma-showers. This is because the lower momentum particles are less difficult to spread than the high energy particles.

To see how the charge dependence of equations 3.1 contributes to the change of EAS images we displayed the ground distributions caused by the electrons (figure 11) and positrons (figure 12) of the EAS. Comparing these figures and equations 3.1 we can see that the pairs e^-/e^+, which give rise to the Cherenkov photons in γ-like showers, are spreaded in opposite directions along the EAS enlargement direction. If we include the charge sign in equations 3.1 we can see that for each azimuth angle the light distribution in the corresponding ground distribution plot in figures 11 and 12 is spreaded in the direction given by the unity vectors on the equation.

All these simulations have been done for two fixed zenith angles (15^o and 45^o) which represents only the low and high zenith angle cases. All the conclusions fix with what we explained on section 1, so we should expect the higher effect between North ($\phi = 180$) and South ($\phi = 0$) directions and at zenith angle closer to 50^o.

From this analysis we see that the magnetic field will affect the light density collected by the telescope as well as the shower image parameters in the case of imaging telescopes ([12]). In the following section we will concentrated only on the decrease of the light density and therefore the decrease of the effective area.

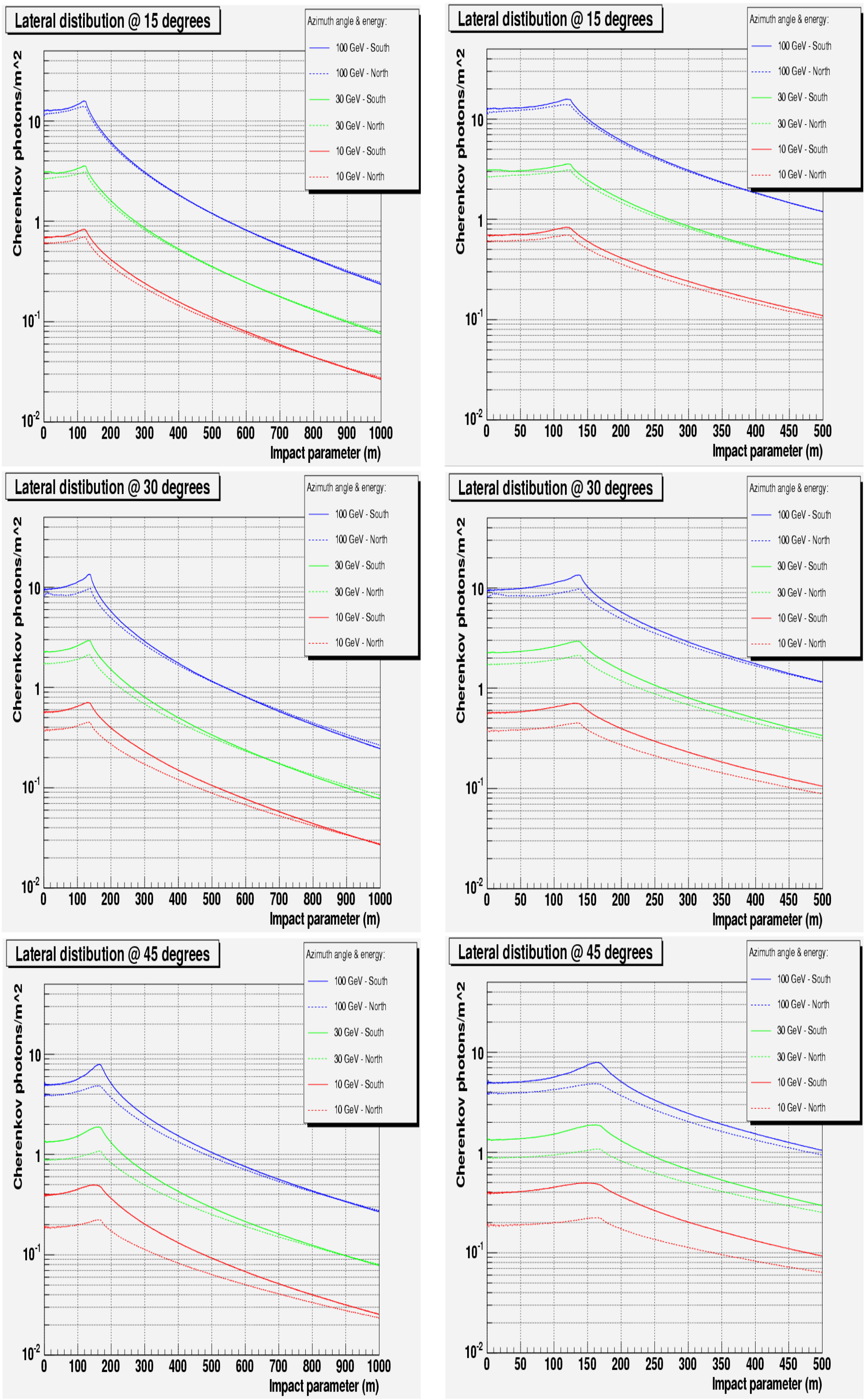

Figure 9: *Lateral distribution of Cherenkov photons for gamma showers of 10, 30 and 100 GeV and zenith angles of 15, 30 and 45 degrees. Right plots are zoom of the left ones for impact parameter up to 500 meters.*

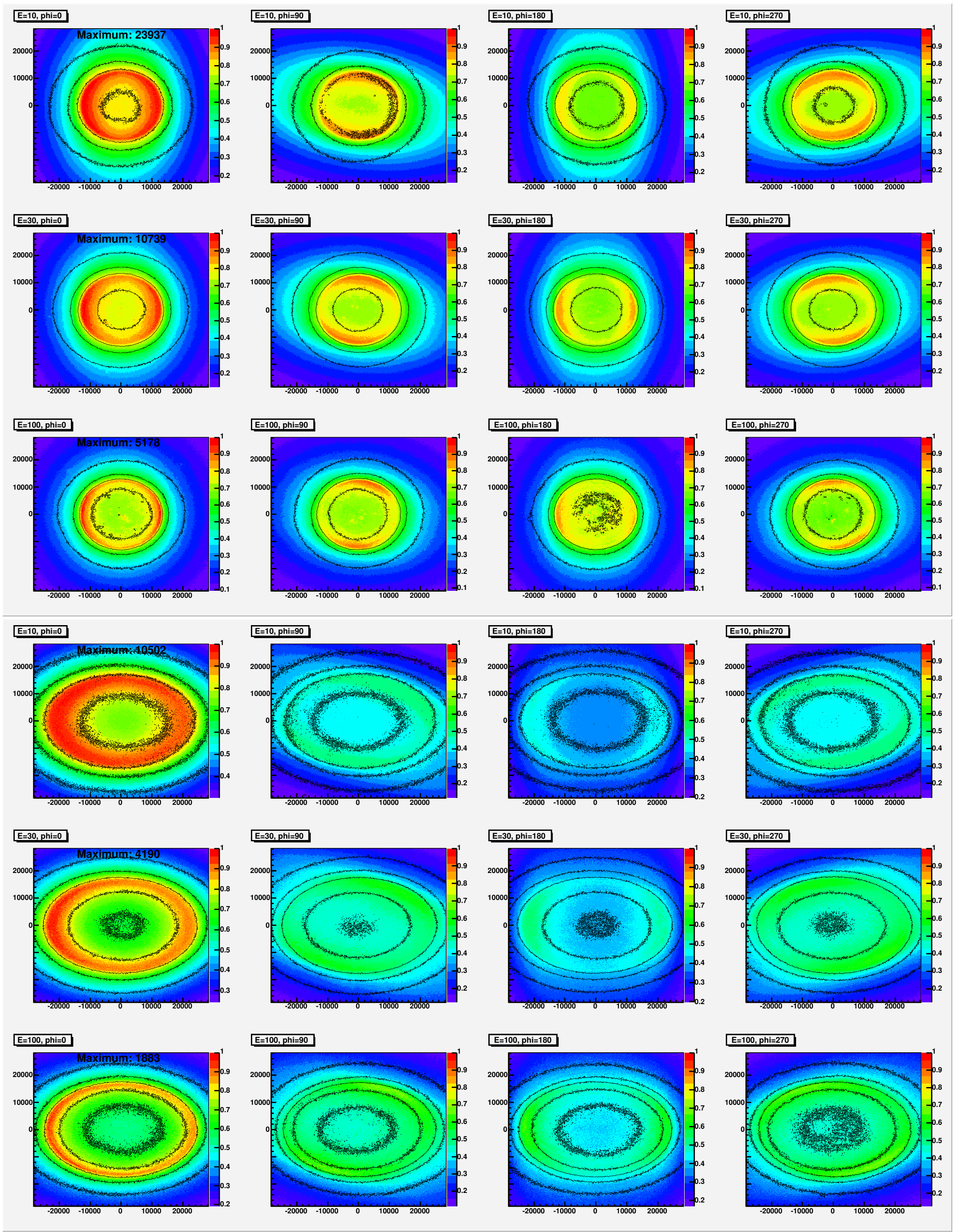

Figure 10: *Ground distribution of Cherenkov photons for gamma showers (all components) of 10, 30 and 100 GeV and zenith angles of 15 and 45 degrees. Color plot correspond to EAS with B field while in contour plots the B field is not simulated.*

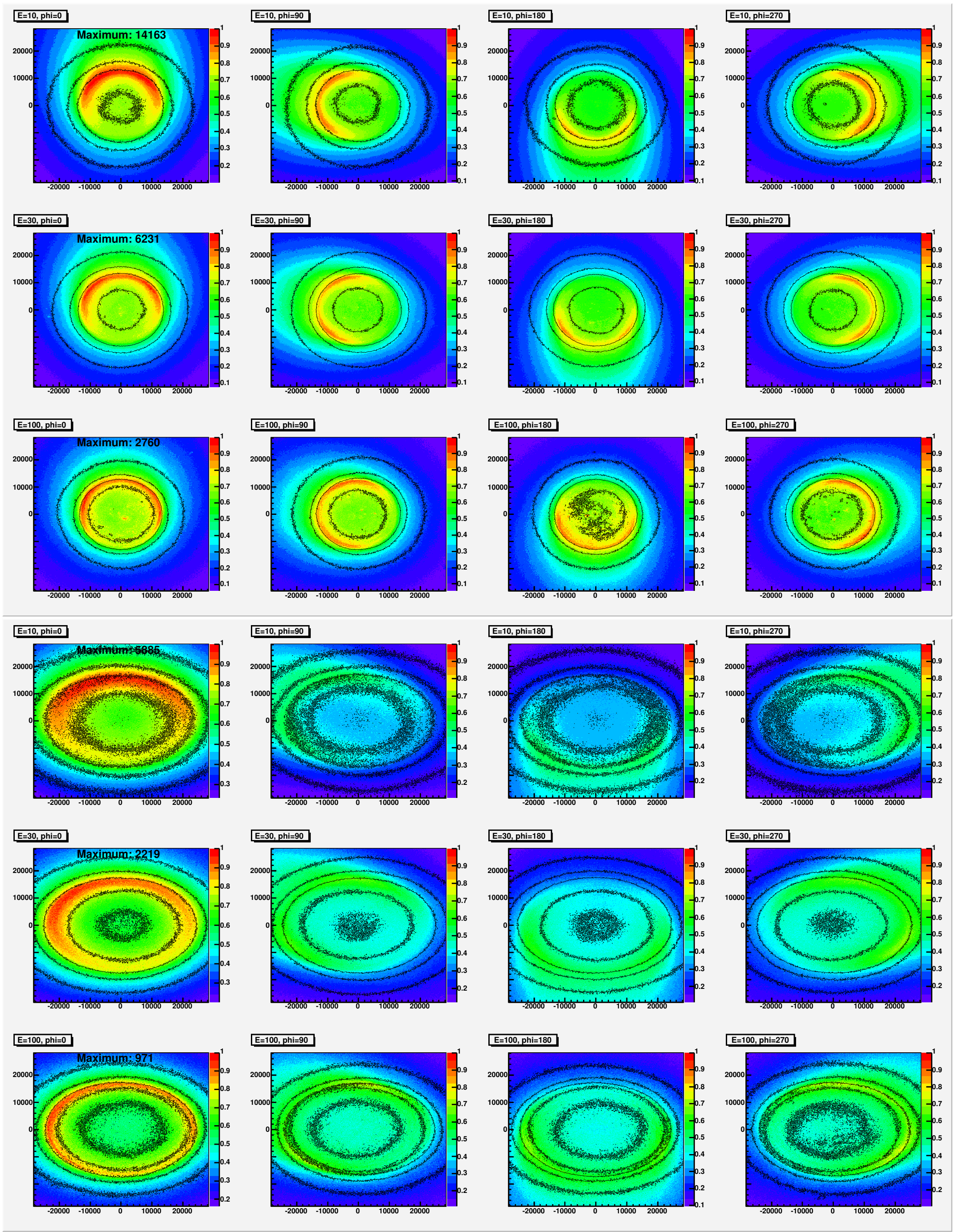

Figure 11: *Ground distribution of Cherenkov photons for gamma showers (electron component) of 10, 30 and 100 GeV and zenith angles of 15 and 45 degrees. Color plot correspond to EAS with B field while in contour plots the B field is not simulated.*

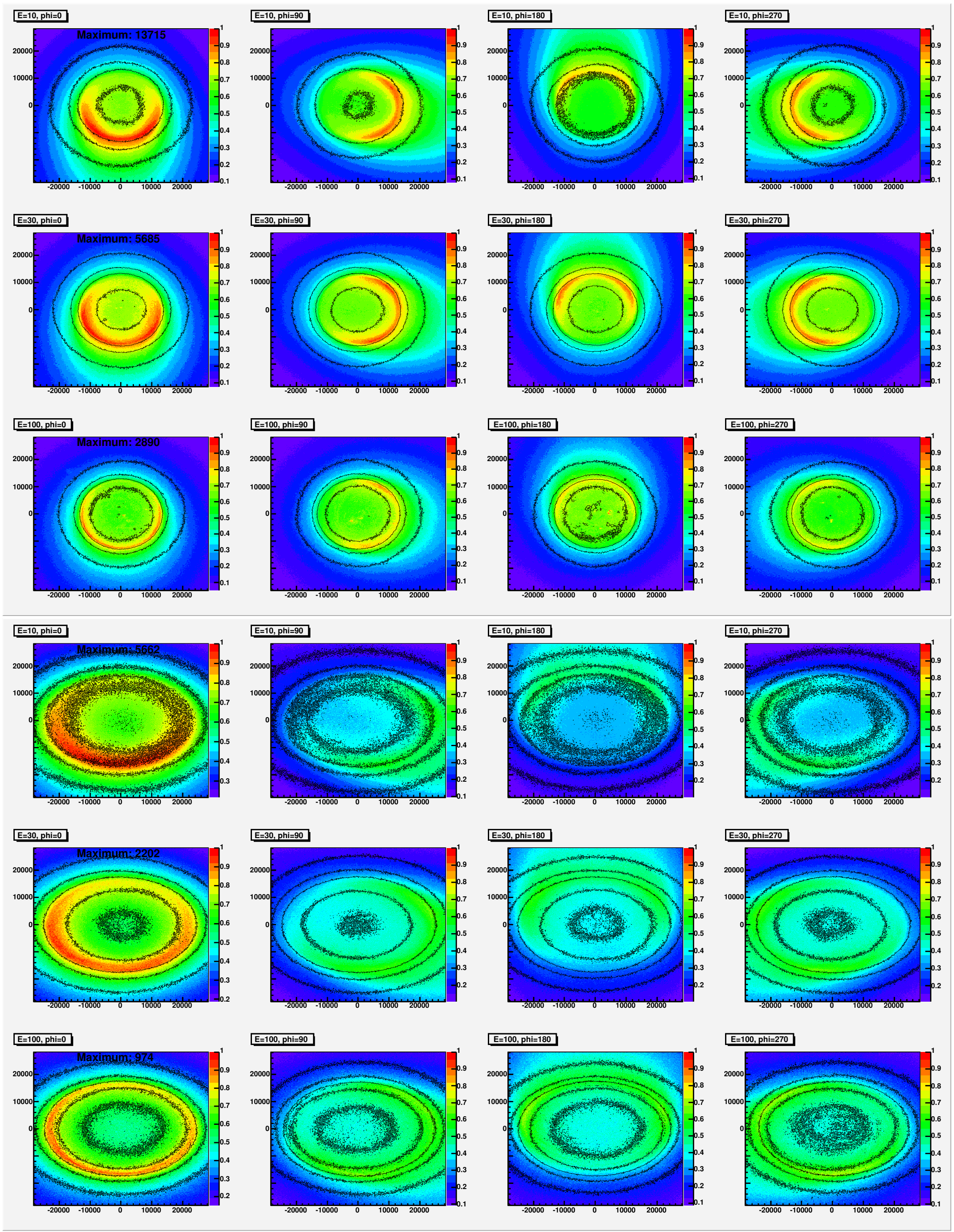

Figure 12: *Ground distribution of Cherenkov photons for gamma showers (positron component) of 10, 30 and 100 GeV and zenith angles of 15 and 45 degrees. Color plot correspond to EAS with B field while in contour plots the B field is not simulated.*

3.2 Effective areas

As we saw previously when one considers the North direction, there is a lost of Cherenkov photons, up to 50%, for low energies and high zenith angles with respect to the South. This drives us to consider the possibility of a decrease in the trigger efficiency and also in the effective area.

As we explained in section 2, we can calculate a rough approximation to the effective collection area at different energies and zenith angles (see figure 13).

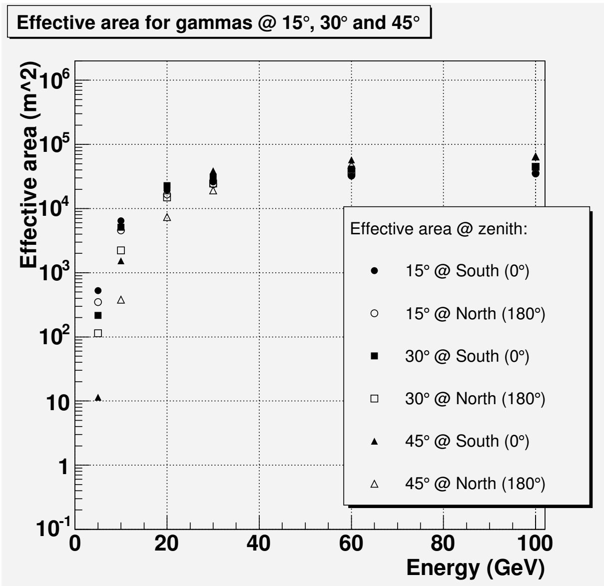

Figure 13: *Effective area for gammas for energies of 5, 10, 20, 30, 60 and 100 GeV at zenith angles of 15, 30 and 45 degrees.*

In figure 13 we show the effective area for North and South directions as a function of the energy of the gamma showers. The variation at different energies and zenith angles are shown in table 3. The general shape of the curve resembles the results obtained with the full simulation, and can therefore give an indication of the relative differences between North and South until a more detailed study is available. The comments made with respect to the lateral distributions apply also here to the effective areas: the effect of the magnetic field increases with zenith angle and decreases with energy.

	15 º	30º	45º
5 GeV	30%	60%	90%
10 GeV	30%	60%	70%
20 GeV	20%	40 %	70%
30 GeV	10%	30%	70%
60 GeV	4%	5%	30%
100 GeV	~0%	1%	10%

Table 3: *Relative difference in the effective area between North (empty marker) and South (filled marker) (figure 13) direction for gamma showers of energy 5, 10, 20, 30, 60 and 100 GeV and zenith angles of 15, 30 and 45 degrees.*

3.3 Proposed setup for Montecarlo simulations

As we saw previously, due to the fact that the effective area changes with the azimuth angle, it will be necessary to simulate Montecarlo data at different angles. Our goal is to find the best set of azimuth angles for the MC simulations.

Since the magnetic field effect is higher at low energies, we have represented the effective area for 15, 30 and 45 degrees of zenith angle as a function of the $B_\perp$ and different azimuth angles (figure 14) for gamma showers of 30 GeV.

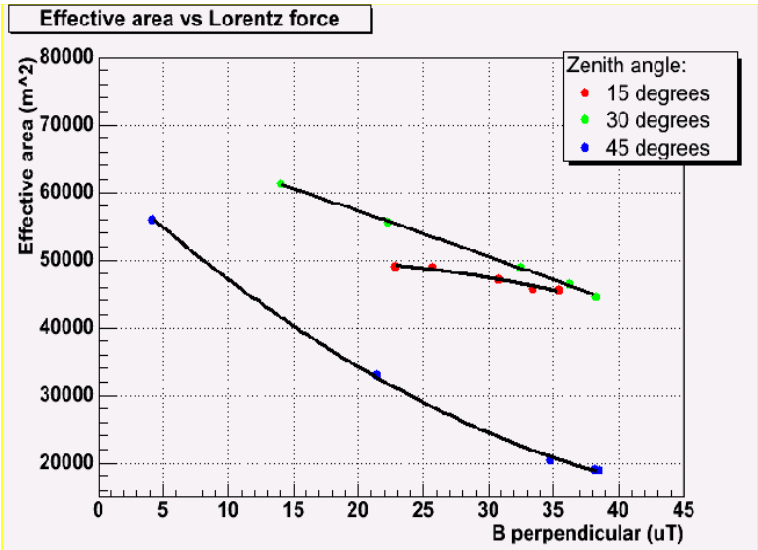

Figure 14: *Effective area versus the $B_\perp$ at La Palma for different zenith (15°, 30° and 45°) and azimuth (0°, 45°, 90°, 120° and 180°) angles for gamma showers of 30 GeV.*

It can be seen that the effective area changes slowly with the $B_\perp$ (equation 3). The rate of change depends on the zenith angle. For equally spaced points in the $B_\perp$ of around 11 μT the effective area changes between 5 - 30%, depending on the zenith angle. We have fitted the curves with a second order polynomial, also shown in figure 14.

$$|\vec{B_\perp}| = \{B_z^2 \sin^2\theta \sin^2\phi + (B_x \cos\theta - B_z \sin\theta \sin\phi)^2 + B_x^2 \sin^2\theta \sin^2\phi\}^{1/2} \tag{3}$$

In MAGIC, the Montecarlo simulations have been done with different zenith angles equally spaced in solid angle of generation ($\Delta\Omega = 2\pi\Delta(\cos\theta)$) where $\Delta(\cos\theta) = 0.01$. For each of these generation bins we have defined a number of azimuth ($B_\perp$) bins using $N_{bins} = (F_{max} - F_{min})/(\Delta F)_{max}$, rounded to the nearest integer. $(\Delta F)_{max}$ is the maximum increment in $B_\perp$, and was set to 11 μT, chosen to have a reasonable number of bins in the last zenith angle generated, and at least three bins everywhere. Since the range of values of $B_\perp$ depends on the zenith angle (see figure 3) the number of azimuth angle bins also depends on it. The used formulae are:

$$\begin{aligned} |\vec{B_\perp}|_{min} &= B_x \cos\theta - B_z \sin\theta \\ |\vec{B_\perp}|_{max} &= \begin{cases} B_x \cos\theta + B_z \sin\theta, & \theta < 38^o.7 \\ \{B_x^2 + B_z^2\}^{1/2}, & \theta > 38^o.7 \end{cases} \end{aligned}$$

Once we have calculated the number of $B_\perp$ bins, the azimuth angle values are calculated. The increment in $B_\perp$ is $\Delta|\vec{B_\perp}| = (B_{\perp,max} - B_{\perp,min})/N_{bins}$ and the corresponding azimuth angle for each $B_\perp$ bin is $\cos\phi = \frac{-B_z\cos\theta + \sqrt{B_x^2 + B_z^2 - |\vec{F}|^2}}{B_x \sin\theta}$
The generation azimuth angles that we propose for each zenith angle bin can be seen in table 4. The value of the effective area for any zenith angle can then be obtained by interpolation.

Bin	θ(°)	$\Delta|\vec{B_\perp}|$	ϕ(°)
0	0.00	0.0	0, 180
1	8.11	6.8	0, 180
2	11.48	9.6	0, 180
3	14.07	5.9	0, 75, 180
4	16.26	6.8	0, 73, 180
5	18.19	7.6	0, 71, 180
6	19.95	8.3	0, 69, 180
7	21.57	8.9	0, 68, 180
8	23.07	9.5	0, 66, 180
9	24.49	10.1	0, 65, 180
10	25.84	10.6	0, 64, 180
11	27.13	7.4	0, 46, 80, 180
12	28.36	7.7	0, 45, 79, 180
13	29.54	8.0	0, 44, 78, 180
14	30.68	8.2	0, 43, 76, 180
15	31.79	8.5	0, 42, 75, 180
16	32.86	8.8	0, 41, 74, 180
17	33.90	9.0	0, 41, 73, 180
18	34.92	9.3	0, 40, 72, 180
19	35.90	9.5	0, 39, 70, 180
20	36.87	9.7	0, 38, 69, 180
21	37.81	9.9	0, 37, 68, 180
22	38.74	10.1	0, 36, 67, 180
23	39.65	10.3	0, 36, 66, 165
24	40.54	10.5	0, 35, 65, 160
25	41.41	10.7	0, 34, 64, 155
26	42.27	10.9	0, 33, 63, 152
27	43.11	8.3	0, 26, 46, 72, 149
28	43.95	8.5	0, 25, 46, 71, 146
29	44.77	8.6	0, 24, 45, 70, 144
30	45.57	8.7	0, 24, 44, 69, 141
31	46.37	8.9	0, 23, 43, 68, 140

Table 4: *Proposed generation azimuth angle for each zenith angle bin of the Montecarlo simulation.*

4 Protons

4.1 Lateral distributions

As we have seen, in the case of gammas, $B_\perp$ affects to the electromagnetic sub-cascades of the EAS development.

In the case of the proton particle, when it interacts with the atmospheric atoms, the first three particles of the EAS are pions (π^0,π^+ and π^-). The π^0 particle gives rise to electromagnetic subcascades which, as we saw in the case of gammas, will produce the Cherenkov photons. The two charged pions gives rise to other charged and not charged particles when they interacts with the atmospheric atoms, several of them produce also electromagnetic subcascades but in less amount than the π^0. Among these charged particles there are mouns which also produce Cherenkov photons.

Due to the fact that there are more charged particles which produce Cherenkov light and that two of the three main particles produced in the first interaction of protons EAS are charged, we expect to have also an effect of the Earth's magnetic field into the protons showers. We have calculated the effect of $B_\perp$ in the charged particles of the proton showers. With the same method described in the gamma section we have generated proton showers (table 5) at different energies and zenith angles coming from the North and South directions.

Energy / Zenith angle	Number of events		
	15 °	30°	45°
30 GeV	10^4	10^4	10^4
300 GeV	10^4	10^4	10^4
3 TeV	10^2	10^2	10^2

Table 5: *Number of proton showers generated for each azimuth angle (North and South) as a function of energy and zenith angle.*

The protons come isotropically from all sky directions and normally all the protons inside a view cone of 5 degrees are considered. This would include photons comming from different directions in the lateral distribution. Since the magnetic field depends on the direction where the primary particle come from we have generated protons showers coming from a punctual source.

In figure 15 we have represented the lateral distribution of Cherenkov photons for proton showers at different energies and zenith angles for North and South directions. As we expected, the Cherenkov light density decreases with energy, zenith angle and increases with the impact parameter. The curve for proton showers of 30 GeV is not as well defined as at the other energies, due to the low amount of Cherenkov photons produced at these energies.

The difference in the light density between North and South directions is not so relevant as in the case of gammas. This is better seen in the three plots on the right, a zoom up to 500 meters of impact paramenter of the left ones. At energies of 30 GeV the density of Cherenkov photons is very low and fluctuations are important. At energies around 300 GeV and 3 TeV it seems to be a little difference between North and South directions, but it is very small and appears to depend not much with the energy or zenith angle of the primary proton.

Comparing with gamma showers (figure 9) we can see that gamma showers of 100 GeV and proton showers of 300 GeV have the same density of Cherenkov photons at low impact parameters. But apart from this, the proton showers do not show any difference in the amount of Cherenkov photons between

North and South directions, while the gamma showers experiment a decrease of around 50% at zenith angles of around 45°.

These plots are the integral of all the light for each impact parameter bin. Although there is hardly no effect of the perpendicular component of the magnetic field in the lateral distribution of proton showers, as well as in the case of gamma-showers, it could be expected that the magnetic field affects the shape and size of the EAS ground distribution being the dispersion effect relevant within each impact parameter bin. The ground distribution has been represented in figures 16, 17 and 18. As in the gamma shower section, in these figures the color scale plots correspond to EAS simulated with La Palma magnetic field values and the contour lines plots are the corresponding ones where no non magnetic field has been applied.

In these figures (16, 17 and 18) it is shown the ground distribution of Cherenkov photons for proton showers of 30 GeV, 300 GeV and 3 TeV at zenith angle of 15° (on the top) and 45° (on the bottom) for different pointing directions S(ϕ=0), E(ϕ=90), N(ϕ=180) and W(ϕ=270). All of them are normalized to the maximum value (displayed in a label) of the distribution in the South direction ($\phi = 0$) where the minimum effect of the magnetic field is expected (figure 3). Figure 16 shows the light distribution from all the charged particles of the proton EAS, figure 17 shows the light distribution due to electrons and figure 18 from positrons.

It is supossed that the magnetic field will have the same effect on the electromagnetic subcascades from proton showers than on gamma showers, because there isn't any difference between them. The only difference is that in gamma showers they come from $\gamma - > e^+/e^-$ processes while in proton showers they come from π^0 desintegration process.

Due to this we could expect that the upper plots (low zenith angles) in figures 16, 17 and 18 doesn't show any effect of the magnetic field, as in gamma EAS distributions. If we take a look to this plot we can see that the shape of the shower, through all the pointing directions, remains the same for proton energies of 300 Gev and 3 TeV. In the case of 30 GeV proton showers, it is not possible to perfom any analysis due to the low statistic of Cherenkov photons which doesn't give rise to any clear image.

In the case of shower images at zenith angle of 45° all the images extend along the X-axis due to the projection of the shower image to the telescope reference frame, as in the case of gamma showers, but there is not any change on the shower shape depending on the pointing direction (azimuth angle).

As in the case of gamma showers we can see that in proton showers the Cherenkov light density increase with the energy and decrease with the zenith angle. In both figures, 16 and 15, we see that the only difference in azimuth angle is a decrease of the Cherenkov photons for proton showers coming from North direction. But this difference it very small. To see if this is due to the magnetic field we have plotted the ground distribution for proton showers in color scale for the simulation without magnetic field. This can be seen in the figures 19, 20 and 21.

In this figures we see that the light distributions at ground have the same shape and size that in the case of applied B. The difference comes only in the light density but thi difference is very small and due to fluctuations in the own shower because at high zenith angles (45°), for energies of 30 and 300 GeV the light density is bigger with B than without, and the opossite for 3 TeV.

For these reasons we can conclude that the Earth's magnetic field doesn't have any effect into the light density coming from proton showers.

Trying to find an explanation to this we come back to the fact that in proton showers several charged particles (e^-/e^+ and muons) emit Cherenkov light. So we have simulate also the light distributions and the ground distributions coming from electron/positron pairs (green) and the rest of particles, mainly muons, (blue). This can be seen in figure 22. We have represent primary protons of 300 Gev and 3 TeV coming from North and South directions at zenith angle of 45^o, at which it is expected a higher effect from the Earth's magnetic field. We have excluded the 30 GeV protons showers due to the low statiscs and the large fluctuations seen previously. We can see from the three plots that at all the energies the mean contribution to the total photon density comes from the Cherenkov photons created by electron/positron pairs (green lines).

From these plots we can see clearly that the electromagnetic cascades (e^-/e^+) are the main contributors to the total Cherenkov light emitted by a proton shower. We can see that also the electronic component of the light density have a different light distribution between North and South directions. Since the muons have small momenta, they are less disturbed and only the the electron/positron component of the proton showers is affected by the Earth's magnetic field.

Looking the plots in figure 22 we can see that, as it was expected, the effect of the Earth's magnetic field depends on the amount of electron/positron pairs, as in the case of gamma showers. Although it seems that there is a negligible effect in the light density, we could expect to have any effect in the distribution of Cherenkov photons in the telescope plain coming from electrons or positrons. These distributions are shown in figures 17 and 18. In these plots the effect of the magnetic field is seen in the dispersion direction of each e^-/e^+ component, which coincides with the γ-like showers. But in the case of proton showers most of their Cherenkov photons are emitted at low impact parameters and the electron/positron pairs are widely distributed so the effect of the perpendicular component of the magnetic field is lower.

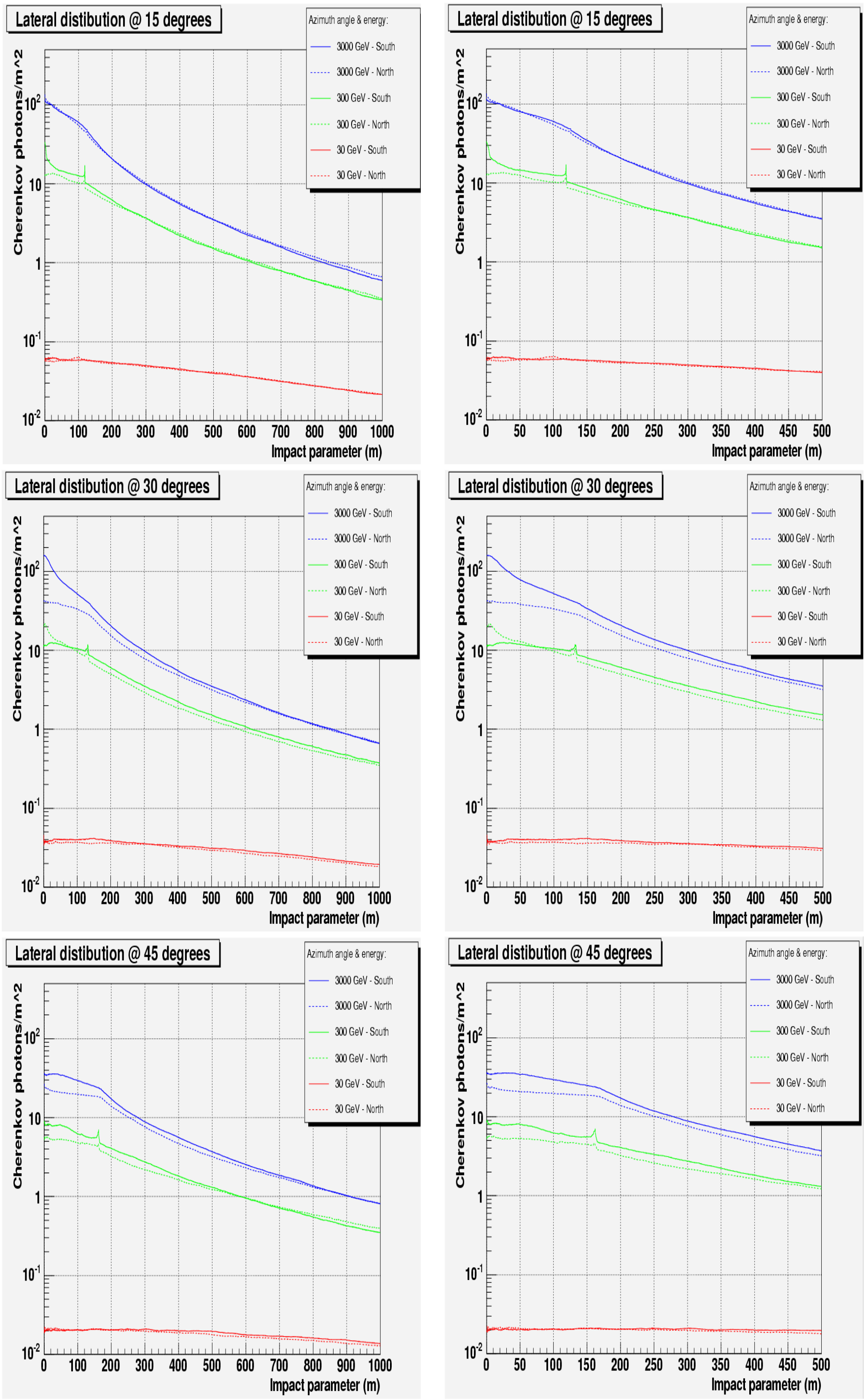

Figure 15: *Lateral distribution of Cherenkov photons for proton showers of 30, 300 and 3000 GeV and zenith angles of 15, 30 and 45 degrees. Right plots are zoom of the left ones for impact parameter up to 500 meters.*

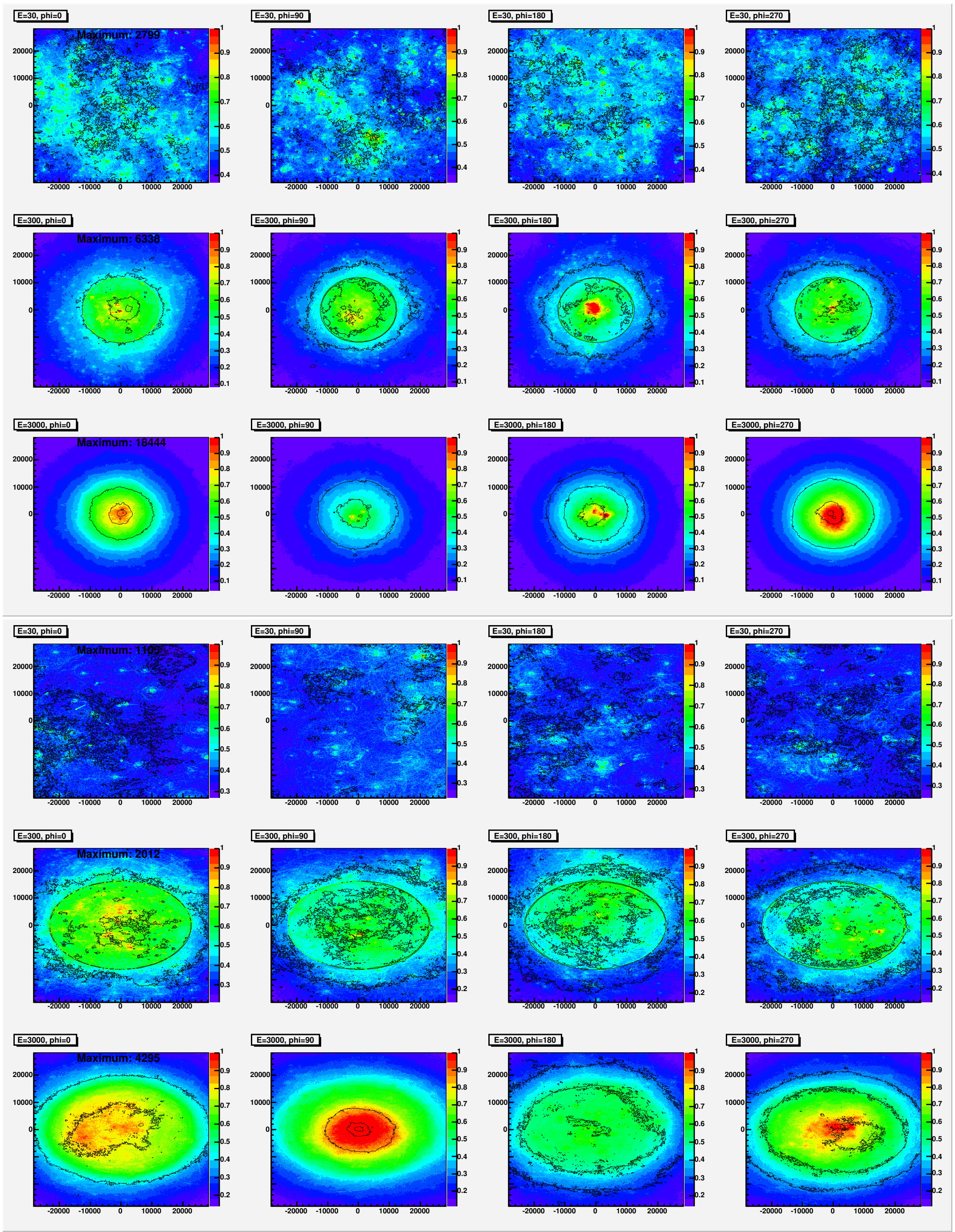

Figure 16: *Ground distribution of Cherenkov photons for proton showers (all components) of 30, 300 and 3000 GeV and zenith angles of 15 and 45 degrees. Color plot correspond to EAS with B field while in contour plots the B field is not simulated.*

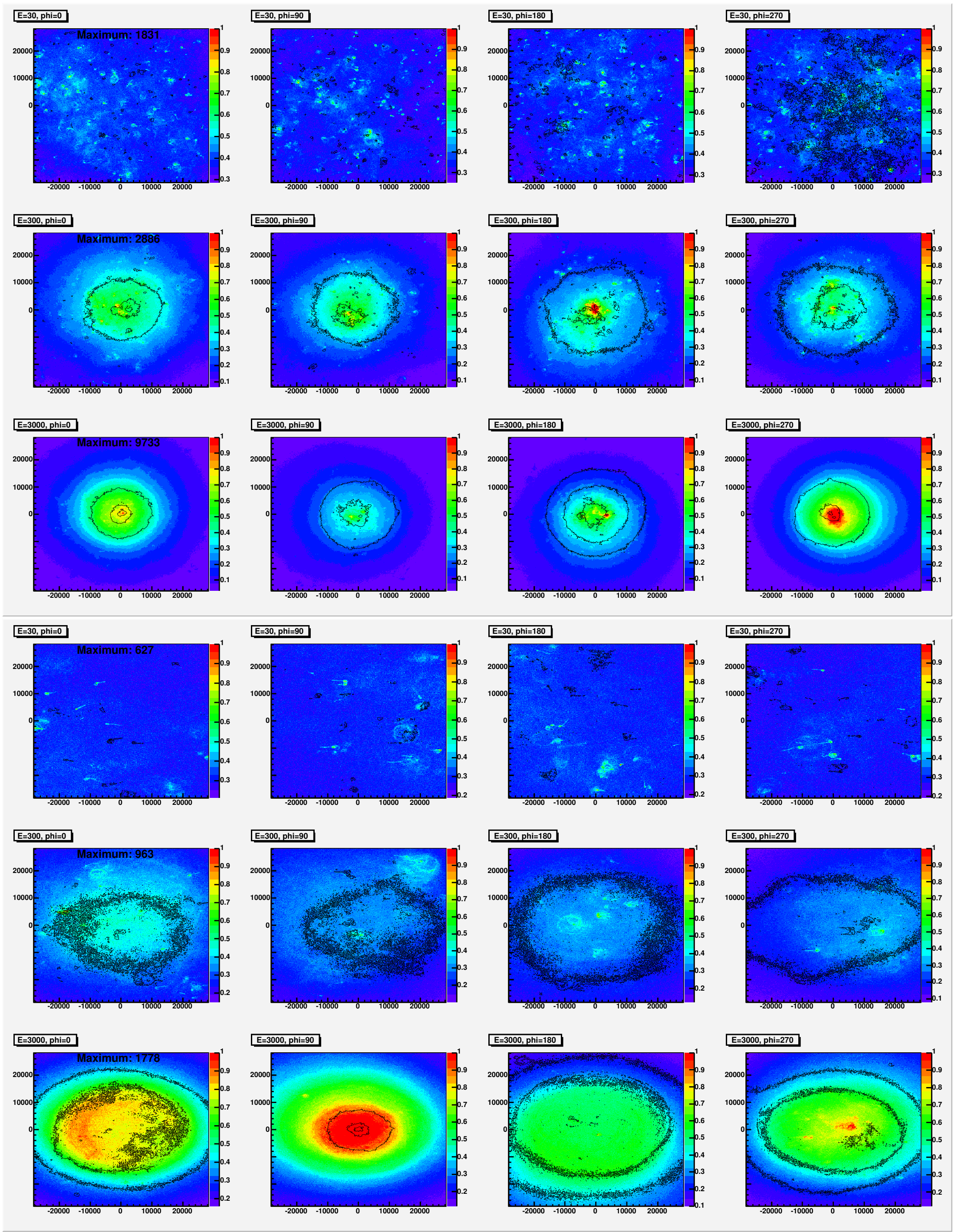

Figure 17: *Ground distribution of Cherenkov photons for proton showers (electron component) of 30, 300 and 3000 GeV and zenith angles of 15 and 45 degrees. Color plot correspond to EAS with B field while in contour plots the B field is not simulated.*

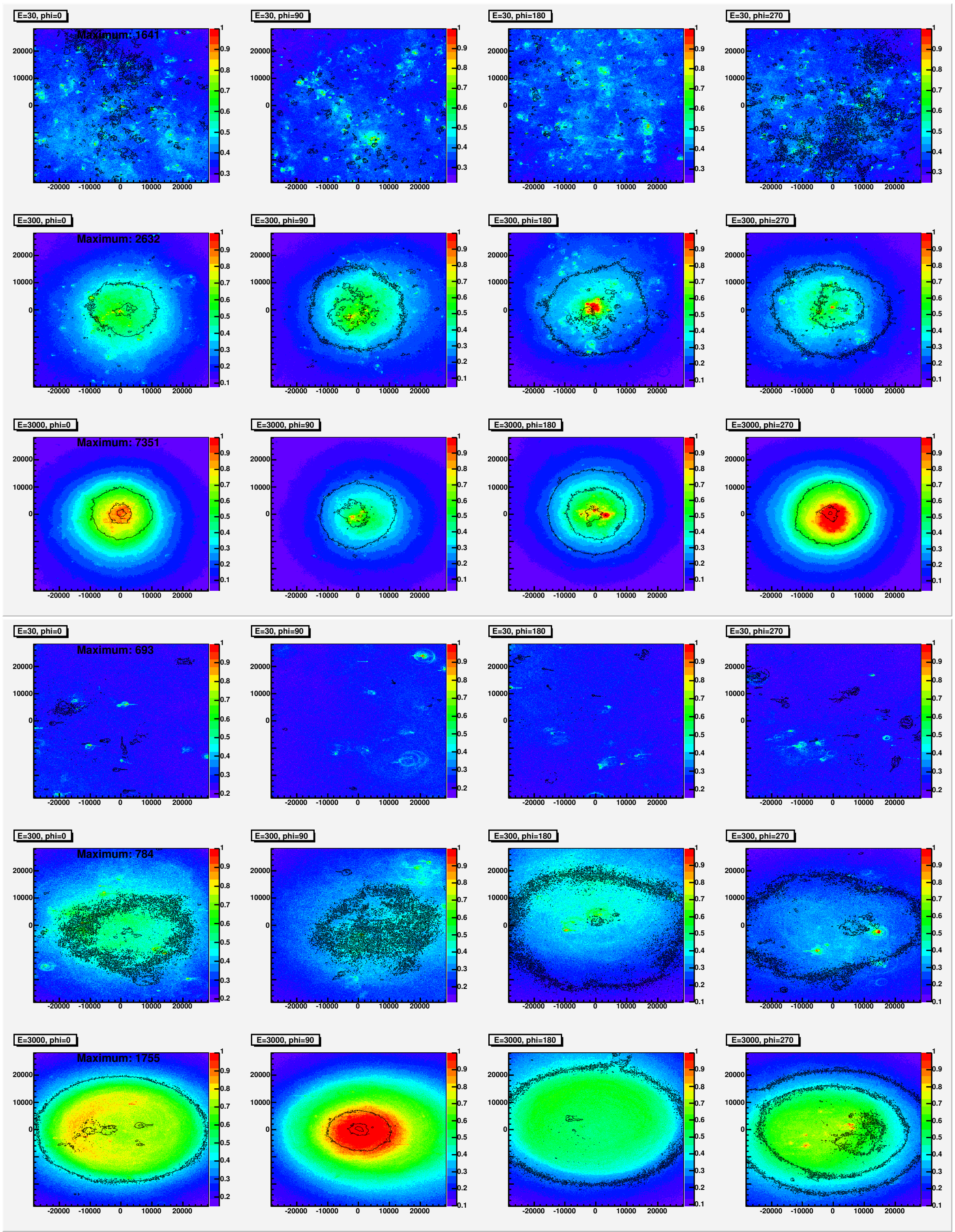

Figure 18: *Ground distribution of Cherenkov photons for proton showers (positron component) of 30, 300 and 3000 GeV and zenith angles of 15 and 45 degrees. Color plot correspond to EAS with B field while in contour plots the B field is not simulated.*

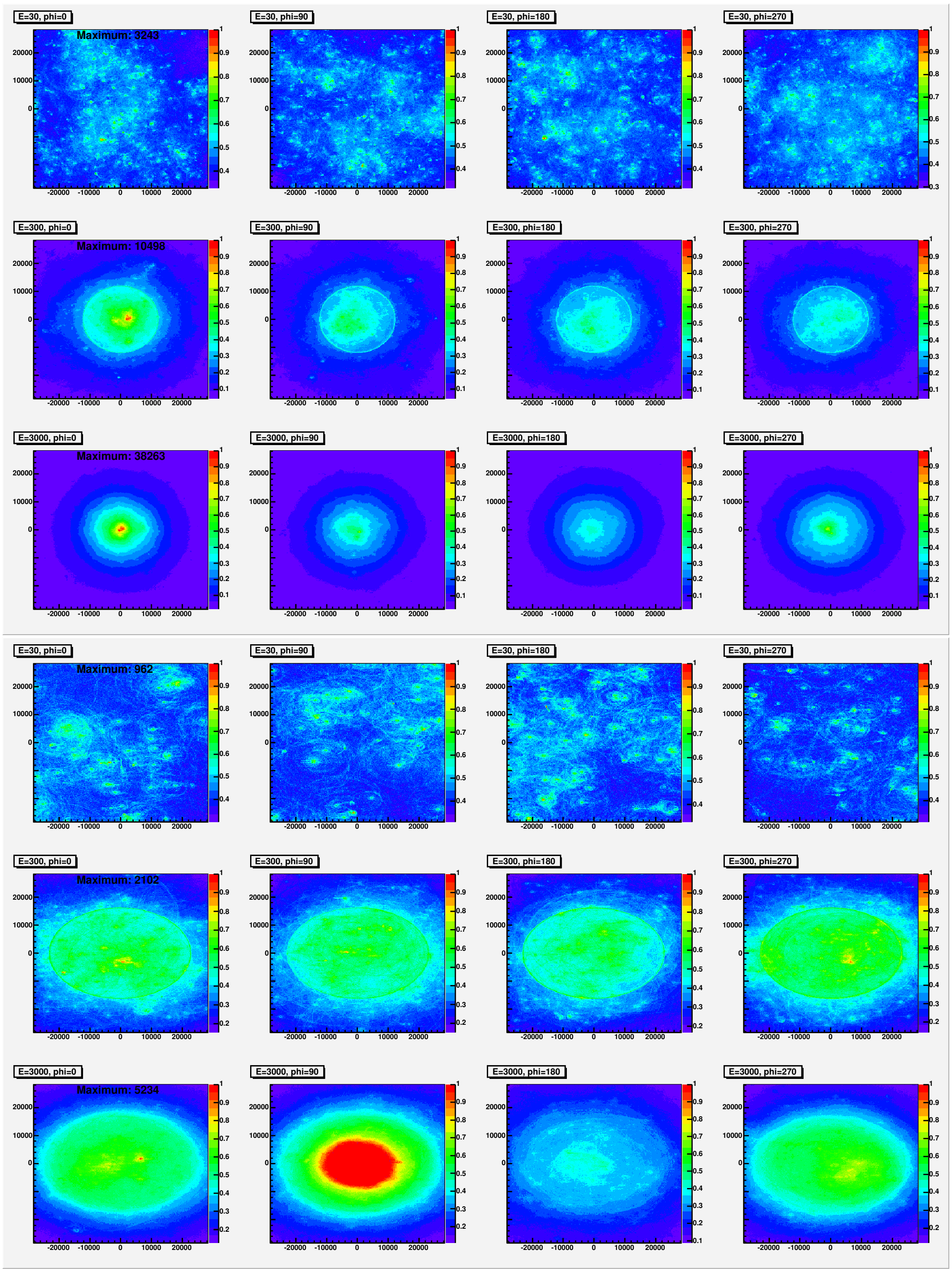

Figure 19: *Ground distribution of Cherenkov photons for proton showers (all components) without B of 30, 300 and 3000 GeV and zenith angles of 15 and 45 degrees.*

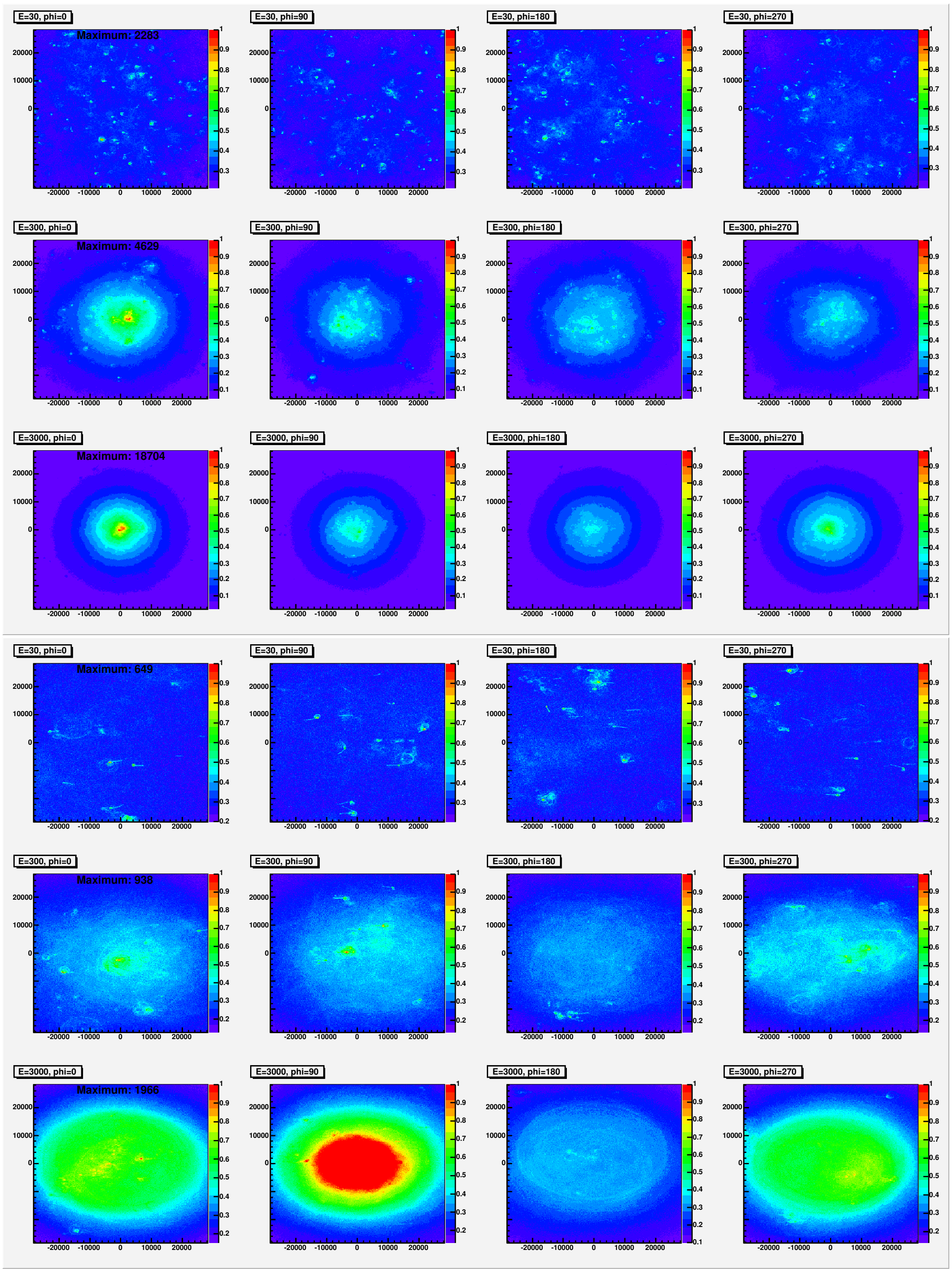

Figure 20: *Ground distribution of Cherenkov photons for proton showers (electron component) without B of 30, 300 and 3000 GeV and zenith angles of 15 and 45 degrees.*

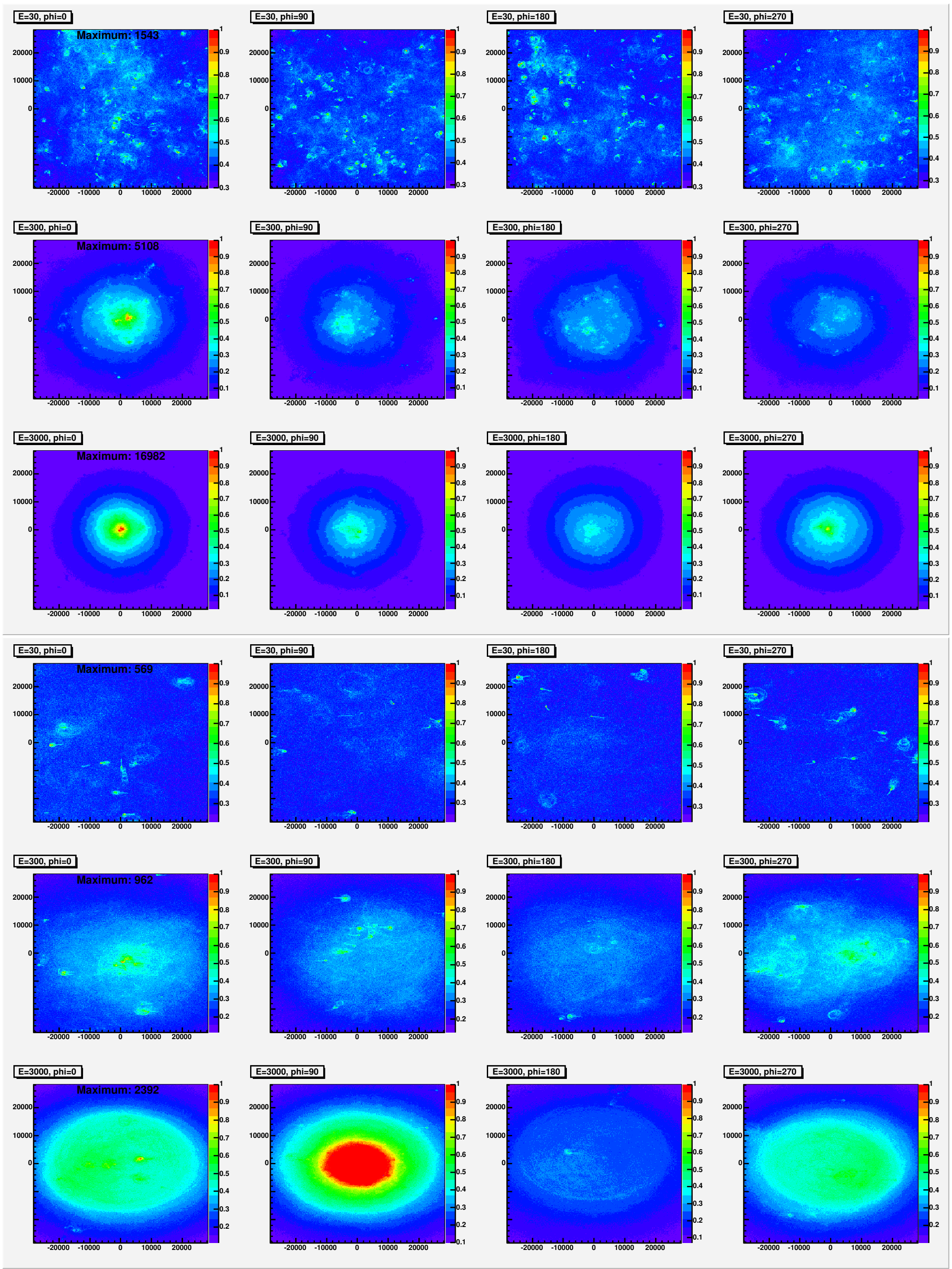

Figure 21: *Ground distribution of Cherenkov photons for proton showers (positron component) without B of 30, 300 and 3000 GeV and zenith angles of 15 and 45 degrees.*

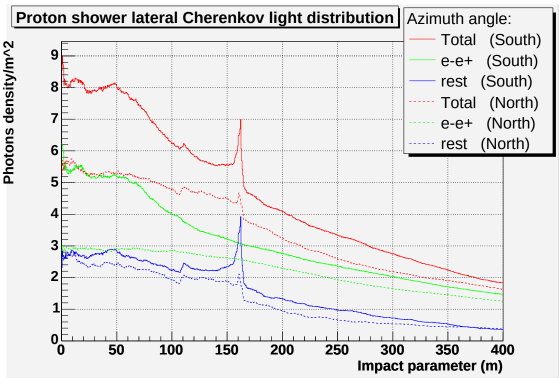

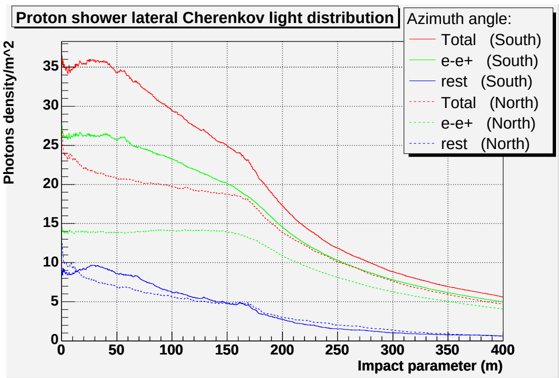

Figure 22: *Lateral distribution components in proton showers of 300 (left) and 3000 GeV (right) at zenith angle of 45°.*

4.2 Effective areas

With the same method as in gamma showers, we have calculated the proton effective area. As we can see in figure 23 the proton sensitivity does hardly change with the energy and zenith angle, as we have shown in the lateral distributions.

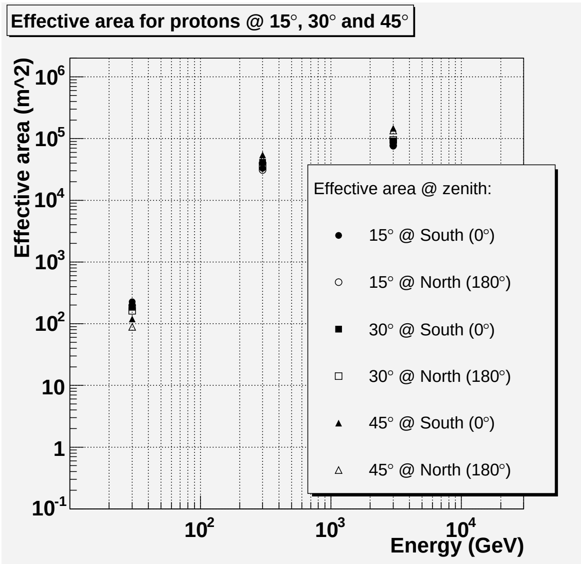

Figure 23: *Effective area for protons at energies of 30, 300 and 3000 GeV zenith angles of 15, 30 and 45 degrees.*

5 Conclusions and outlook

From this study we can conclude that the effect of the magnetic field in the showers development has to be taken into account depending on the observation site and telescope threshold, having different importance for different places.

In the case of MAGIC (La Palma), the effect is important for gammas at high zenith angles ($\geq 30^o$) and low energies (≤ 100 GeV), while for protons the effect is not significant. This has to be considered for pulsar studies, since pulsar spectra have low cutoffs, up to 50 GeV or 100 GeV (depending on the model) and most of the pulsed component is assumed to arise from the energy range between 10-40 GeV.

As the energy thresholds of future planned telescopes diminish, magnetic field effects will become more important. We think this effect will be very important for future upgrades of MAGIC.

We have proposed a binning for the Montecarlo simulation for gamma showers, which uses azimuth angles equally spaced in the perpendicular component of magnetic field. In this way azimuth angle dependent corrections can be computed. For low energies they might be very important.

In the case of the background we have to consider also the energy cutoff of the magnetic field in the charged particles (mainly protons ([8]) and electrons ([9])). This makes that charged particles below an energy (cutoff energy) the charged particles does not reach the atmosphere. The protons with energy higher than the magnetic cutoff are not affected in their shower development. For electrons with enough energy, the effect of the magnetic field in their lateral distribution is similar to gamma showers, due to the similar behavior in the development of both particle showers.

Finally we want to point out some open directions in which we think this work continue:

- This work should include studies on the effect of B on the image parameters to yield a more complete view of the influence of B on Magic results (see [10] and [12]).
- Implement this study for future upgrades of MAGIC and next generation of 30 m Cherenkov telescopes.

References

[1] *http://www.ngdc.noaa.gov/cgi-bin/seg/gmag/fldsnth1.pl*.

[2] *http://hegra1.mppmu.mpg.de/MAGICWeb/Intro.html*.

[3] *http://www.mpi-hd.mpg.de/htm/HESS/HESS.html*.

[4] *http://linmax.sao.arizona.edu/help/FLWO/whipple.html*.

[5] *http://icrhp9.icrr.u-tokyo.ac.jp/intro.html*.

[6] *http://www.tuc.nrao.edu/alma/site/chajnantor/maps/coordinates.html*.

[7] F.A. Aharonian, A.K. Konopelko, H.J. Völk, *5@5 - a 5 GeV energy threshold array of imaging atmospheric Cherenkov telescopes at 5 km altitude*, 2001, Astroparticle Physics, 15, 4, 335-356.

[8] Biland, A., 2003, ECO meeting (Barcelona).

[9] Cortina, J. and Gonzalez, J.C., 2001, Astro. Phys., 15(2), 203-210.

[10] M.Kasztelan, T.Wibig, D.Sobczynska, MAGIC-TDAS 02-13, 021217/TWibig, 17 December 2002.

[11] J. Knapp, D. Heck, *Extensive Air Shower Simulation with CORSIKA: A User's Guide*, Institut für Kernphysik, Forschungszentrum Karlsruhe GmbH, November 8, 1995.

[12] A. Wenger, *The effect of the earth magnetic field on extensive air showers*, Diploma thesis, Institute for Particle Physics, ETH Zürich. March, 2004.